Analytical Description of Transmembrane Voltage Induced by Electric Fields on Spheroidal Cells

Tadej Kotnik and Damijan Miklavčič

Faculty of Electrical Engineering, University of Ljubljana, SI-1000 Ljubljana, Slovenia

Analytical Description of Transmembrane Voltage Induced by Electric Fields on Spheroidal Cells

Tadej Kotnik and Damijan Miklavčič

Faculty of Electrical Engineering, University of Ljubljana, SI-1000 Ljubljana, Slovenia

ABSTRACT   An analytical description of transmembrane voltage induced on spherical cells was determined in the 1950s, and the tools for numerical assessment of transmembrane voltage induced on spheroidal cells were developed in the 1970s. However, it has often been claimed that an analytical description is unattainable for spheroidal cells, while others have asserted that even if attainable, it does not befit the reality due to the nonuniform membrane thickness, which is unrealistic but inevitable in spheroidal geometry. In this paper we show that for all spheroidal cells, membrane thickness is irrelevant to the induced transmembrane voltage under the assumption of a nonconductive membrane, which was also applied in the derivation of Schwan's equation. We then derive the analytical description of transmembrane voltage induced on prolate and oblate spheroidal cells. The final result, which we cast from spheroidal into more familiar spherical coordinates, represents a generalization of Schwan's equation to all spheroidal cells (of which spherical cells are a special case). The obtained expression is easy to apply, and we give a simple example of such application. We conclude the study by analyzing the variation of induced transmembrane voltage as a spheroidal cell is stretched by the field, performing one study at a constant membrane surface area, and another at a constant cell volume.

INTRODUCTION

Placement of a biological cell into an electric field leads to a local distortion of the field in the cell and in its vicinity. As the conductivity of the cell membrane is several orders of magnitude lower than those of the cytoplasm and the physiological extracellular medium, most of the electric field within the cell is concentrated on the membrane. In a DC field, the induced transmembrane voltage reaches the steady state within microseconds after the start of the exposure. For the treatment of the transients, the reader is referred to Kotnik et al. (1998), while in this work we henceforth deal only with the steady-state situation.

Analytical description of steady-state transmembrane voltage induced on spherical cells was derived more than four decades ago by H. P. Schwan (Schwan, 1957). To simplify the derivation, Schwan assumed the membrane to be nonconductive, which led to the well-known relation, often referred to as the (steady-state) Schwan's equation

$$\Delta\Phi = \tfrac{3}{2} ER \cos \varphi, \qquad (1)$$

where $\Delta\Phi$ is the induced transmembrane voltage, E is the external electric field, R is the cell radius, and φ is the polar angle measured from the center of the cell with respect to the direction of the field. With physiological values of the conductivities, $\Delta\Phi$ as given by Eq. 1 differs at most by several parts per thousand from the exact result given by

(see, e.g., Kotnik et al., 1997):

$$\Delta\Phi = \frac{3}{2} \frac{\sigma_{\mathrm{e}}[3dR^2\sigma_{\mathrm{i}} + (3d^2R - d^3)(\sigma_{\mathrm{m}} - \sigma_{\mathrm{i}})]}{\begin{bmatrix} R^3(\sigma_{\mathrm{m}} + 2\sigma_{\mathrm{e}})(\sigma_{\mathrm{m}} + \tfrac{1}{2}\sigma_{\mathrm{i}}) \\ - (R - d)^3(\sigma_{\mathrm{e}} - \sigma_{\mathrm{m}})(\sigma_{\mathrm{i}} - \sigma_{\mathrm{m}}) \end{bmatrix}} ER \cos \varphi$$

$$(2)$$

where σ_{i}, σ_{m}, and σ_{e} are electric conductivities of the cytoplasm, cell membrane, and external medium, respectively, and d is the membrane thickness (note that this equation applies only in the case of a membrane of constant thickness and conductivity). It is easy to check that setting $\sigma_{\mathrm{m}} = 0$ leads to cancellation of d, σ_{i}, and σ_{e} from Eq. 2, which thereby simplifies into Eq. 1.

In the 1970s, this knowledge was extended by the development of methods for numerical calculation of transmembrane voltage induced on spheroidal cells (Klee and Plonsey, 1972, 1976). Despite that, an analytical description of the transmembrane voltage induced on spheroidal cells, if attainable, would give a deeper insight than numerical calculations can provide.

The search for an analytical solution in spheroidal geometry has often been claimed futile (Bernhardt and Pauly, 1973; Klee and Plonsey, 1976; Gimsa and Wachner, 1999): as we show in this paper, rather unfoundedly. This claim was motivated by the fact that for analytical determination of the induced transmembrane voltage, cell boundaries must coincide with coordinate surfaces of some coordinate system. In spheroidal coordinate systems, this necessarily renders a membrane of nonuniform thickness, which is unrealistic. Still, two recent papers treated an analytical solution for prolate spheroids. The first paper gave an expression for the electric potential inside and outside a prolate spheroid with a nonconductive membrane (Bryant and Wolfe, 1987), and the second paper generalized the result to the case of a

conductive membrane (Jerry et al., 1996). Nevertheless, in both studies the results are formulated in prolate spheroidal coordinates, thus lacking the insight that is available in the more familiar spherical coordinates. To our knowledge, no similar work has been published on oblate spheroids, although these represent a suitable model for some types of cells, such as erythrocytes. In summary, an analog of Schwan's equation (1) for spheroidal cells has not yet been given.

In this work we first show that under the assumption of a nonconductive membrane, the induced transmembrane voltage is unaffected by membrane thickness as long as the cell is symmetrical with respect to a plane to which the field is perpendicular. Analytical calculation of the induced transmembrane voltage is therefore justified and valid, and in the Appendices we derive the transmembrane voltage induced on both prolate and oblate spheroidal cells. To allow for comparison with Schwan's equation, we present the results in spherical coordinates, where a spheroid is described by its two radii, and the location on the membrane is given—as for a sphere—by the polar angle measured from the center of the spheroid with respect to the direction of the field.

METHODS

Derivation of the steady-state induced transmembrane voltage

Let the presence of the cell distort a homogeneous electric field $\mathbf{E}_0$ into an electric field $\mathbf{E}$. To determine the steady-state induced transmembrane voltage, we express $\mathbf{E}$ in terms of the electric potential Φ

$$\mathbf{E} = -\nabla\Phi, \tag{3}$$

where Φ satisfies Laplace's equation

$$\nabla^2\Phi = 0 \tag{4}$$

with the following conditions:

1. homogeneity of the field far from the cell,

$$\lim_{r\to\infty}(-\nabla\Phi) = \mathbf{E}_0; \tag{5a}$$

2. finiteness of the potential inside the cell,

$$\lim_{r\to 0}\Phi < \infty; \tag{5b}$$

3. continuity of the potential and the current density at the boundary surfaces between the cytoplasm and the membrane and between the membrane and the exterior,

$$(\Phi_i - \Phi_m)|_{\mathscr{S}_i} = 0,$$

$$\mathbf{n}\cdot(\sigma_i\nabla\Phi_i - \sigma_m\nabla\Phi_m)|_{\mathscr{S}_i} = 0,$$

$$(\Phi_m - \Phi_e)|_{\mathscr{S}_e} = 0, \tag{5c}$$

$$\mathbf{n}\cdot(\sigma_m\nabla\Phi_m - \sigma_e\nabla\Phi_e)|_{\mathscr{S}_e} = 0,$$

where $\mathscr{S}_i$ and $\mathscr{S}_e$ are the inner and the outer membrane surface; Φ_i, Φ_m, and Φ_e denote the function Φ in the cell interior, the membrane, and the cell

exterior; σ_i, σ_m, and σ_e are the conductivities of these three regions; and $\mathbf{n}$ is the unit normal vector to the treated boundary surface.

The transmembrane voltage $\Delta\Phi$ induced by the external electric field on the cell membrane is the difference between the values of electric potential at the two boundary surfaces,

$$\Delta\Phi = \Phi|_{\mathscr{S}_i} - \Phi|_{\mathscr{S}_e}. \tag{6}$$

We note that in Eq. 6 and hereafter in this paper, Δ always represents the difference operator and should not be confused with another established notation, $\Delta \equiv \nabla^2$ for the Laplacian operator.

Simplifications for a nonconductive membrane

Due to the shielding effect caused by the low conductivity of the membrane, most of the electric potential variation within the cell occurs in its membrane. In the hypothetical case of a nonconductive membrane, the shielding is complete; there is no electric field in the cytoplasm, and the electric potential variation within the cell occurs only in its membrane.

At this point we introduce the following principle of invariance, which is crucial for further derivations:

For an object with a nonconductive membrane which is placed into a homogeneous electric field,

(i) the electric potential outside the object is determined only by the shape of the object;

(ii) if the object is symmetrical with respect to a plane to which the external field is perpendicular, then also the induced transmembrane voltage is determined only by the shape of the object.

The proof of this principle is given in Appendix A, while Fig. 1 illustrates it by an example. In a given field, the potential outside *A*, *B*, *C*, and *D* is the same. For objects *B*, *C*, and *D* that are symmetrical with respect to a plane to which the field is perpendicular (*dotted vertical*), the electric potential in the interior, and thus the transmembrane voltage, is also the same (for *D*, which consists entirely of a nonconductive material, we define the transmembrane voltage as the difference between the values of the electric potential in its center and on its surface).

For a spherical cell, part (ii) of the principle of invariance stated above is clearly demonstrated by Eq. 1, which involves the cell radius, but not the membrane thickness. For spheroidal cells, validity of (ii) is similarly confirmed by Eq. 7, introduced in the next subsection.

For cells with planar symmetry and with a nonconductive membrane, the thickness of the membrane is therefore irrelevant to the induced transmembrane voltage, which can be determined by solving Laplace's equation for any object with planar symmetry and the same external shape. In Fig. 1, all objects have the same, prolate spheroidal external shape. With a uniform membrane thickness, object *B* is a realistic model of a cell, but its internal membrane surface is not a prolate spheroid, and Laplace's equation cannot be solved analytically. Unlike that, the two surfaces of *C* and the surface of *D* are all prolate spheroids, and for these two objects Laplace's equation is solvable in prolate spheroidal coordinates by separation of variables. By assigning the potential $\Phi = 0$ to the plane of symmetry, the transmembrane voltage induced on *B* then equals the opposite of the electric potential calculated at the external surface of either *C* or *D*.

In summary, for a cell with planar symmetry and a nonconductive membrane, the induced transmembrane voltage can be determined analytically given that 1) the cell shape can be modeled as a coordinate surface in some coordinate system, and 2) Laplace's equation is separable in this coordinate system. These two requirements are both necessary and sufficient, and 2) provides a restriction to 14 different coordinate systems (Eisenhart, 1934; Morse and Feshbach, 1953). The spherical, the prolate spheroidal, and the oblate spheroidal coordinate systems are among these, and we now proceed to the derivation and analysis of the transmembrane voltage induced on spheroidal cells.

RESULTS AND DISCUSSION

Transmembrane voltage induced on spheroidal cells

Because of its extent, the detailed derivation of the transmembrane voltage induced on a spherical, a prolate spheroidal, and an oblate spheroidal cell with the axis of rotational symmetry parallel to the field is given in Appendices B–D. Written in spherical coordinates, the final result reads

$$\Delta\Phi(\varphi) = \begin{cases} E\,\dfrac{R_2^2 - R_1^2}{\dfrac{R_2^2}{\sqrt{R_2^2 - R_1^2}}\,\mathrm{arccot}\,\dfrac{R_1}{\sqrt{R_2^2 - R_1^2}} - R_1} & R_1 < R_2 \\[6pt] \qquad\times\,\dfrac{R_2\cos\varphi}{\sqrt{R_1^2\sin^2\varphi + R_2^2\cos^2\varphi}}; & \\[10pt] \frac{3}{2}ER_1\cos\varphi = \frac{3}{2}ER_2\cos\varphi; & R_1 = R_2 \\[10pt] E\,\dfrac{R_1^2 - R_2^2}{R_1 - \dfrac{R_2^2}{\sqrt{R_1^2 - R_2^2}}\,\log\dfrac{R_1 + \sqrt{R_1^2 - R_2^2}}{R_2}} & R_1 > R_2 \\[6pt] \qquad\times\,\dfrac{R_2\cos\varphi}{\sqrt{R_1^2\sin^2\varphi + R_2^2\cos^2\varphi}}; & \end{cases}$$

(7)

where E is the external electric field, R_1 is the radius along the axis of rotational symmetry (the polar radius), R_2 is the radius perpendicular to this axis (the equatorial radius), and φ is the polar angle measured from the center of the cell with respect to the direction of the field.

As an example of the application of Eq. 7, in Fig. 2 we plot the function $\Delta\Phi(\varphi)$ for three spheroids with different equatorial radii, but with the same polar radius.

Unlike with a sphere, the arc length on the membrane of a general spheroid is not proportional to the angle φ. The normalized arc length $p(\varphi)$ is defined as

$$p(\varphi) = \frac{\int_0^{\arctan(R_1/R_2\,\tan\varphi)} \sqrt{R_1^2\sin^2\phi + R_2^2\cos^2\phi}\,d\phi}{\int_0^{2\pi} \sqrt{R_1^2\sin^2\phi + R_2^2\cos^2\phi}\,d\phi}.$$

(8)

This does not allow for an explicit expression of $\varphi(p)$—and thus also of $\Delta\Phi(p)$—but they can be calculated by means of numerical mapping of p onto φ. The graph shown in Fig. 3 is analogous to the one in Fig. 2, showing $\Delta\Phi(p)$ instead of $\Delta\Phi(\varphi)$.

Figs. 2 and 3 imply that the shape of a spheroid determines not only the maximum value of $\Delta\Phi$, but also the fraction of the membrane which is exposed to high values of $\Delta\Phi$. The induced transmembrane voltage close to the maximum value occupies only a small region of the membrane in very prolate, "cigar-shaped" cells, and a much larger region in very oblate, "disk-shaped" cells.

A generalization of these examples is given in Fig. 4, which shows, for a given R_1, the maximum value of $\Delta\Phi$ as a function of R_2. With decrease of R_2 this function approaches an infimum of ER_1, but it has no upper bound, and with increase of R_2 it can reach an arbitrarily large value. Still, $\max(\Delta\Phi)$ increases less than proportionally with R_2, and for any $R_2 > 2.32R_1$, $\max(\Delta\Phi) < ER_2$.

Variation of the induced transmembrane voltage with electromechanical deformation

Besides their general applicability, the formulae of Eq. 7 enable an evaluation of the variation of the induced transmembrane voltage that accompanies the electromechanical deformation of the cell in the electric field. The polarization of the cell membrane produces an electric force that acts on the membrane, and as a result the cell is elongated in the direction of the field (Bryant and Wolfe, 1987). Spherical cells are deformed into prolate spheroids, and for most realistic situations we could start from a sphere and analyze the variation of the induced transmembrane voltage as the cell is elongated. However, a generalization of this study to include oblate spheroids provides several interesting results, and we will thus treat the whole range of spheroids, with a sphere representing a transitional point (obviously, this generalization does not in any way affect the results obtained for prolate spheroids). Two distinct conditions can be imposed to hold during the deformation:

1. a constant membrane surface area, S, where

$$S = \begin{cases} 2\pi R_2\left(R_2 + \dfrac{R_1^2}{\sqrt{R_2^2 - R_1^2}}\,\mathrm{arcsinh}\,\dfrac{\sqrt{R_2^2 - R_1^2}}{R_1}\right); & R_1 < R_2 \\[10pt] \qquad\qquad 4\pi R_1 R_2; & R_1 = R_2 \\[10pt] 2\pi R_2\left(R_2 + \dfrac{R_1^2}{\sqrt{R_1^2 - R_2^2}}\,\mathrm{arcsin}\,\dfrac{\sqrt{R_1^2 - R_2^2}}{R_1}\right); & R_1 > R_2 \end{cases}$$

(9)

2. or a constant cell volume, V, where

$$V = \tfrac{4}{3}\pi R_1 R_2^2.$$

(10)

The first requirement is valid for a noncompressible/nonexpansible membrane, and the second one for a nonpermeable membrane (the cytoplasm is largely an aqueous solution, and therefore noncompressible/nonexpansible). The two together cannot hold, since this would render the cell undeformable, while cell elongation in electric fields has been observed repeatedly (Winterhalter and Helfrich, 1988; Neumann and Kakorin, 1996). In reality, neither of the two restrictions holds completely, and since the experimental data are too scarce to either favor or reject any of them, each of them is a possible approximation to the realistic situation. For both, Fig. 5 shows the induced transmembrane voltage as a function of R_1/R_2.
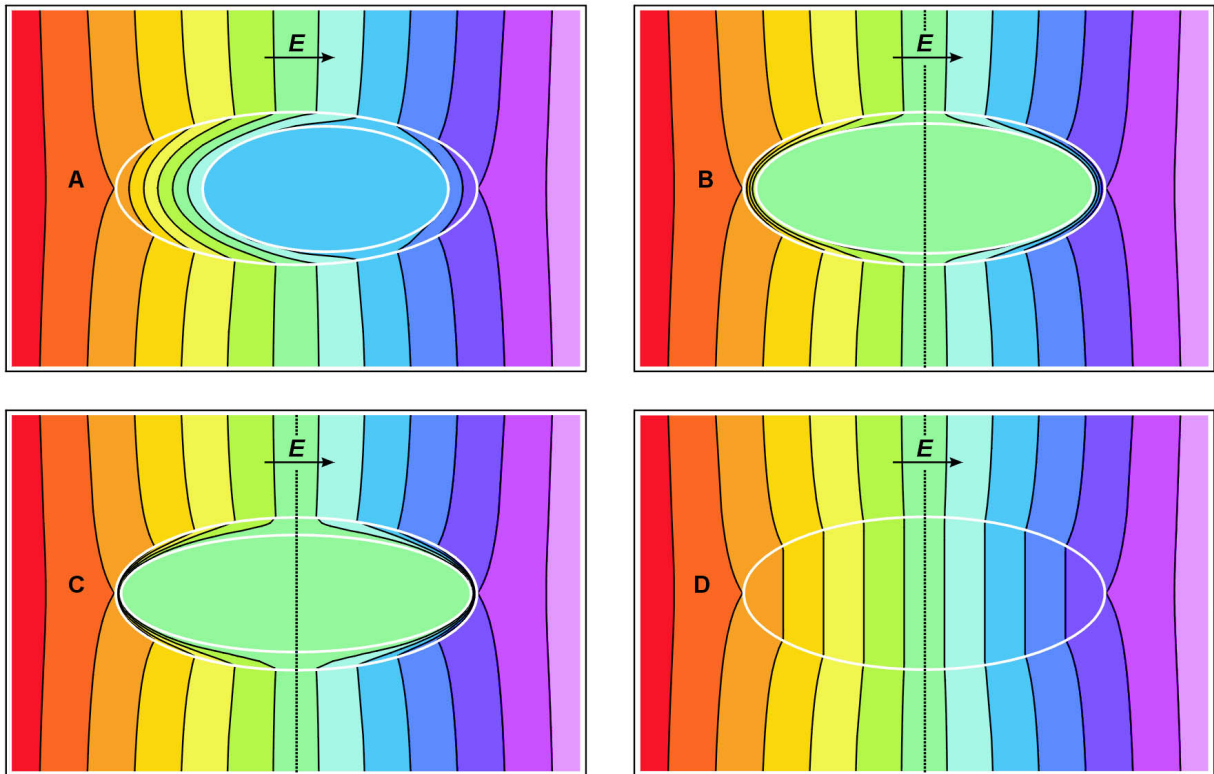
FIGURE 1   Color map of the electric potential outside and inside four objects with different nonconductive membranes, but with identical external shape (in *D*, the membrane fills the object entirely). The potential outside the object is the same for *A*, *B*, *C*, and *D*, while the induced transmembrane voltage is the same for *B*, *C*, and *D*.

Fig. 5 shows that the results under the two restrictions diverge increasingly with cell eccentricity. Nevertheless, deformations into highly eccentrical shapes have never been observed on biological cells, as this is preceded by the membrane rupture (Rand, 1964; Wolfe et al., 1986). Thus, with the exception of naturally highly eccentrical cells (e.g.,
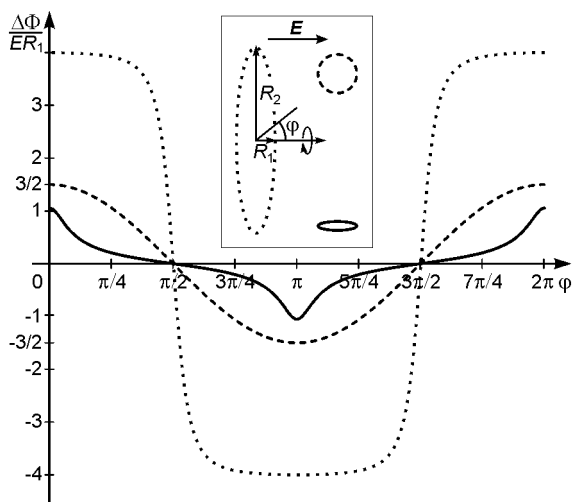

FIGURE 2   The induced transmembrane voltage ( ) in units of ER_1 as a function of the polar angle for three spheroidal cells with equal R_1 and $R_2 = 1/5 R_1$ (*solid line*), $R_2 = R_1$ (*dashed line*), and $R_2 = 5 R_1$ (*dotted line*). *Inset*: the three cells and the field orientation.
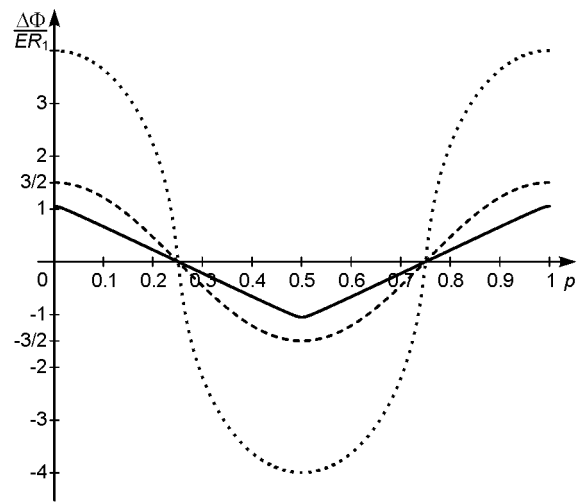

FIGURE 3   The induced transmembrane voltage ( ) in units of ER_1 as a function of the normalized arc length *p* for three spheroidal cells with equal R_1 and $R_2 = 1/5 R_1$ (*solid line*), $R_2 = R_1$ (*dashed line*), and $R_2 = 5 R_1$ (*dotted line*).
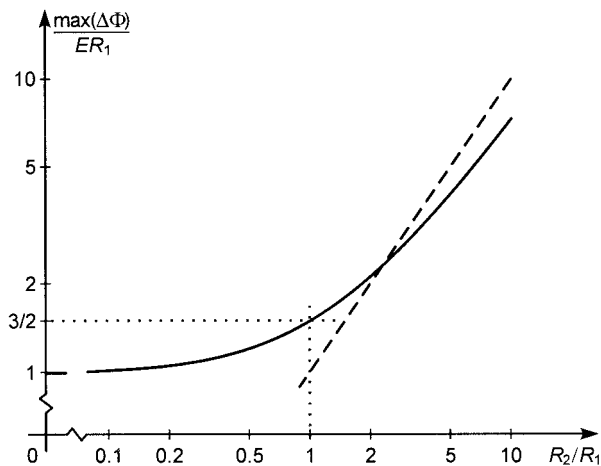
FIGURE 4 The maximum value of the induced transmembrane voltage in units of ER_1 as a function of the ratio R_2/R_1 at a constant R_1 (*solid line*). At $R_2/R_1 = 1$, the cell is a sphere, and the maximum value of the induced transmembrane voltage equals $3/2ER_1$, which is the well-known result also obtained from Schwan's equation. The dashed line shows the value of a hypothetical function $\max(\Delta\Phi) = ER_2$.

bacilli), realistic deformations are in the region where the two radii are of the same order of magnitude. We must also bear in mind that the electric force always tends to elongate the cell in the field direction, and thus for cells that are initially spherical, only the part of Fig. 5 with $R_1/R_2 > 1$ is of practical interest.

CONCLUSIONS

The main result presented in this paper is the analytical description of the transmembrane voltage induced on sphe-
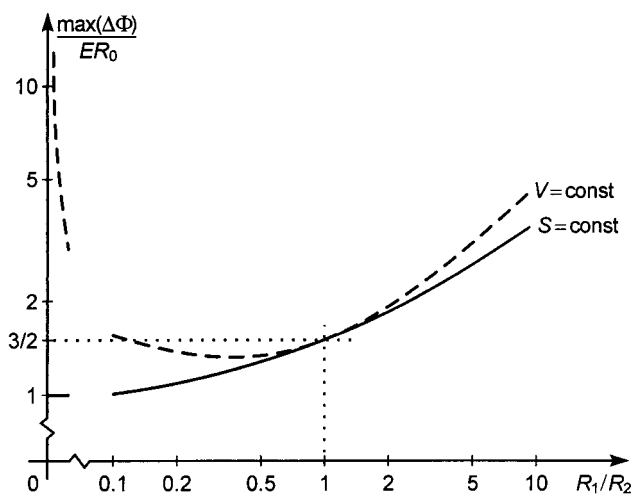

FIGURE 5 The maximum value of the induced transmembrane voltage as a function of the ratio R_1/R_2 with deformation at constant membrane surface area (*solid line*), and at constant cell volume (*dashed line*). Both R_1 and R_2 vary in this study, and we express $\max(\Delta\Phi)$ in units of ER_0, where R_0 is the cell radius at $R_1/R_2 = 1$ (i.e., when the cell is spherical, $R_1 = R_2 = R_0$).

roidal cells, which is given by Eq. 7. Both Schwan's equation and Eq. 7 are derived under the assumption of a nonconductive membrane, and in conditions very far from physiological ones, their validity becomes questionable. In particular, they cannot be applied when cells are suspended in a medium with a conductivity several orders of magnitude below the physiological value, or when the membrane conductivity has been increased by several orders of magnitude, e.g., by electroporation (Grosse and Schwan, 1992; Kotnik et al., 1997). Nevertheless, with the parameter values close to physiological, a variation of membrane thickness by an order of magnitude results in a variation of the induced transmembrane voltage by at most several parts in a thousand, which can be easily checked by means of Eq. 2. Within the range of eccentricities analyzed in this paper, a realistic non-zero conductivity of the cell membrane would therefore have a negligible effect on the induced transmembrane voltage.

It should also be noted that since the presented theory (as well as Schwan's) treats the membrane as a passive conductor, and therefore has a very limited use in excitable cells, such as neurons and muscle fibers, in which the membrane conductivity is in general voltage-dependent.

By itself, Eq. 7 gives a more precise evaluation of the transmembrane voltage induced on various nonspherical cells (erythrocytes, bacteria), but because suspended cells are randomly oriented, analytical results should be accompanied by numerical calculations for various angles between the cell's axis and the field. Nevertheless, the electric field was shown to align prolate cells with their longer axis parallel to the field, and to further elongate these cells, as well as spherical ones (Bryant and Wolfe, 1987; Winterhalter and Helfrich, 1988). Equation 7 is thus valid in the studies of electromechanical cell deformation. In a given field, it determines the electric force, which in equilibrium with the opposing elastic force also defines the shape of the electromechanically deformed cell. By accounting for membrane viscosity as well, one could in principle also evaluate the dynamics of deformation. In addition, since membrane electroporation depends on both the field strength and the membrane curvature (Neumann et al., 1999), a theoretical description of the dynamics of deformation could provide a deeper insight into the mechanisms that accompany (or even facilitate) electroporation.

APPENDIX A

Invariance of Φ and $\Delta\Phi$ for cells with a nonconductive membrane

We treat a general curvilinear coordinate system in $\mathbb{R}^3$, with coordinates ξ_1, ξ_2, ξ_3, in which Laplace's equation is separable. There are 14 such systems (Eisenhart, 1934; Morse and Feshbach, 1953), and in each of these, the physically realistic solution of Laplace's equation can be written in the form

$$\Phi(\xi_1, \xi_2, \xi_3) = Af_1(\xi_1)f_2(\xi_2)f_3(\xi_3) + Bg_1(\xi_1)g_2(\xi_2)g_3(\xi_3),$$

(A.1)

where A and B are the constants determined by the boundary conditions, while f_1, f_2, f_3, g_1, g_2, and g_3 are continuous functions of their variables, bounded everywhere except perhaps at the origin and at infinity. In addition, if a limited number of objects distorts the homogeneity of the field, and the curvilinear coordinates are expressed in terms of spherical coordinates r, φ, and ϑ (see Appendix B), then $f_1(\xi_1(r, \varphi, \vartheta))f_2(\xi_2(r, \varphi, \vartheta))f_3(\xi_3(r, \varphi, \vartheta))$ is a linear function of r.

Let a homogeneous static electric field E_0 permeate the space, and let a single cell, consisting of the cytoplasm and the membrane, be placed into this space. Then, the spatial distribution of the electric potential is given by

$$\Phi(\xi_1, \xi_2, \xi_3)$$

$$= \begin{cases} \Phi_i(\xi_1, \xi_2, \xi_3) & \text{in the cytoplasm} \\ \quad = A_i f_1(\xi_1)f_2(\xi_2)f_3(\xi_3); \\ \\ \Phi_m(\xi_1, \xi_2, \xi_3) & \text{in the membrane} \\ \quad = A_m f_1(\xi_1)f_2(\xi_2)f_3(\xi_3) + B_m g_1(\xi_1)g_2(\xi_2)g_3(\xi_3); \\ \\ \Phi_e(\xi_1, \xi_2, \xi_3) & \text{outside the cell} \\ \quad = -E_0 f_1(\xi_1)f_2(\xi_2)f_3(\xi_3) + B_e g_1(\xi_1)g_2(\xi_2)g_3(\xi_3); \end{cases}$$

(A.2)

This solution satisfies the conditions of electric potential finiteness and electric field homogeneity far from the object, while the conditions of continuity have to be applied to determine the values of the remaining constants. The value of B_e is determined by the continuity of the current density at the external membrane surface ($\mathscr{S}_e$),

$$\mathbf{n} \cdot \sigma_m \nabla\Phi_m|_{\mathscr{S}_e} = \mathbf{n} \cdot \sigma_e \nabla\Phi_e|_{\mathscr{S}_e},$$

(A.3)

where $\mathbf{n}$ is the unit normal vector to the surface $\mathscr{S}_e$, while σ_m and σ_e are the conductivities of the membrane and the external space.

We now assume $\sigma_m = 0$, and Eq. A.3 becomes

$$\mathbf{n} \cdot \nabla\Phi_e|_{\mathscr{S}_e} = 0,$$

(A.4)

and inserting the expression for Φ_e from Eq. A.2 we obtain

$$B_e = E_0 \frac{\mathbf{n} \cdot \nabla(f_1(\xi_1)f_2(\xi_2)f_3(\xi_3))}{\mathbf{n} \cdot \nabla(g_1(\xi_1)g_2(\xi_2)g_3(\xi_3))}\bigg|_{\mathscr{S}_e}.$$

(A.5)

Thus, for a cell with a nonconductive membrane, the value of B_e—and thereby the whole function Φ_e as given by Eq. A.2—is determined solely by the value of E_0 and the shape of the surface $\mathscr{S}_e$.

If the cell is symmetrical with respect to a plane to which the external field far from the cell is perpendicular, the plane of symmetry is an equipotential surface. As Eq. 4 only determines the electric potential up to an additive constant, we assign to this surface—and thereby to the whole cytoplasm—the value of $\Phi = 0$. Eq. 6 then becomes

$$\Delta\Phi = -\Phi|_{\mathscr{S}_e}.$$

(A.6)

Since Eq. A.5 shows that Φ everywhere at the surface $\mathscr{S}_e$ depends only on the electric field and the shape of $\mathscr{S}_e$, Eq. A.6 proves that the induced transmembrane voltage is also determined only by the value of E_0 and the shape of the surface $\mathscr{S}_e$.

APPENDICES B–D

Calculation of $\Delta\Phi$ induced on a spheroidal cell

B. A spherical cell

With a sphere placed into a homogeneous electric field, we derive the spatial distribution of the electric potential in the spherical coordinate system $\{(r, \varphi, \vartheta) \in \mathbb{R}^3 : r \geq 0, 0 \leq \varphi \leq \pi, 0 \leq \vartheta < 2\pi\}$ with the coordinates defined by

$$x = r\cos\varphi, \ y = r\sin\varphi\cos\vartheta, \ z = r\sin\varphi\sin\vartheta.$$

(B.1)

We note that there are several legitimate alternatives in defining the spherical coordinate system, and we choose the one given by Eq. B.1 as it is compatible with the standard notation of r and φ in the circular cylindrical coordinate system $\{(r, \varphi, z) \in \mathbb{R}^3 : r \geq 0, 0 \leq \varphi \leq 2\pi, -\infty < z < \infty\}$. Frequently, notation of φ and ϑ is reversed, or replaced by ϕ and θ, while the Cartesian system is often reoriented with respect to the definitions given above as $(x, y, z) \rightarrow (z, x, y)$.

For geometries with x-axial symmetry, the electric potential is independent of ϑ. We can then write $\Phi(r, \varphi)$ instead of $\Phi(r, \varphi, \vartheta)$, and Laplace's equation reads

$$\frac{\partial^2\Phi}{\partial r^2} + \frac{2}{r}\frac{\partial\Phi}{\partial r} + \frac{1}{r^2}\frac{\partial^2\Phi}{\partial\varphi^2} + \frac{\cot\varphi}{r^2}\frac{\partial\Phi}{\partial\varphi} = 0.$$

(B.2)

The first such case is the electric potential distribution in uniform space. This distribution, which we denote by Φ_0, is linear, and for a field parallel to the x-axis it can be written in spherical coordinates as

$$\Phi_0(r, \varphi) = -Er\cos\varphi.$$

(B.3)

We now place a sphere into this field so that its center coincides with the origin of the coordinate system. Again, we have x-axial symmetry, and by solving for Φ in a separable form

$$\Phi(r, \varphi) = G(r)H(\varphi),$$

(B.4)

Eq. B.2 becomes

$$\frac{r^2 G''(r) + 2rG'(r)}{G(r)} = -\frac{H''(\varphi) + \cot\varphi \, H'(\varphi)}{H(\varphi)}.$$

(B.5)

The left-hand side of Eq. B.5 is at any value of r equal to the right-hand side at any value of φ, which is only possible if they equal the same constant, which we denote by K. This splits Eq. B.5 into two ordinary differential equations

$$\begin{cases} r^2 G''(r) + 2rG'(r) - KG(r) = 0 \\ H''(\varphi) + \cot\varphi \, H'(\varphi) + KH(\varphi) = 0 \end{cases}$$

(B.6)

For $r > 0$, the general solution of the first equation in B.6 is given by

$$G(r) = \begin{cases} C_1 r^{-1/2}\sin\left(\frac{\sqrt{-1-4K}}{2}\log r\right) \\ \quad + C_2 r^{-1/2}\cos\left(\frac{\sqrt{-1-4K}}{2}\log r\right); & K < -\frac{1}{4} \\ \\ C_1 r^{-1} + C_2; & K = -\frac{1}{4} \\ \\ C_1 r^{-1/2(1-\sqrt{1+4K})} + C_2 r^{-1/2(1+\sqrt{1+4K})}; & K > -\frac{1}{4} \end{cases}$$

(B.7)

with C_1, C_2 constants.

Far from the sphere the field is homogeneous, and Eq. B.3 implies that $G(r) \propto r$. Such $G(r)$ is obtained from Eq. B.7 only if $K = 2$, and in that case

$$G(r) = C_1 r + \frac{C_2}{r^2}. \qquad (B.8)$$

For $K = 2$, the equation for $H(\varphi)$ in Eq. B.6 has a solution

$$H(\varphi) = C_3 \cos \varphi + C_4 \left(1 - \cos \varphi \log \sqrt{\frac{1 + \cos \varphi}{1 - \cos \varphi}} \right). \quad (B.9)$$

with C_3, C_4 constants, of which C_4 must be zero, since $H(\varphi)$ is continuous and bounded on $[0, \pi]$, and therefore

$$H(\varphi) = C_3 \cos \varphi. \qquad (B.10)$$

We now join the functions given by Eqs. B.8 and B.10 according to Eq. B.4 and get

$$\Phi(r, \varphi) = Ar \cos \varphi + \frac{B}{r^2} \cos \varphi \qquad (B.11)$$

with A, B constants.

Since we treat the membrane as nonconductive, we proceed as described in the Methods section, looking for the electric potential distribution inside and outside a homogeneous nonconductive sphere. Let $r = R$ describe the surface of the sphere. Both inside and outside the sphere, the electric potential distribution is given by a function of the general form of Eq. B.11, but with different values of A and B. We therefore write

$$\Phi(r, \varphi)$$

$$= \begin{cases} \Phi_i(r, \varphi) = A_i r \cos \varphi + \dfrac{B_i}{r^2} \cos \varphi; & 0 \leq r \leq R \\[3mm] \Phi_e(r, \varphi) = A_e r \cos \varphi + \dfrac{B_e}{r^2} \cos \varphi; & R \leq r \end{cases}$$

$$(B.12)$$

Applying the conditions of continuity and an additional assumption that $\sigma_m = 0$, we get the constants in Eq. B.12,

$$A_i = -\frac{3E}{2},$$

$$B_i = 0,$$

$$A_e = -E, \qquad (B.13)$$

$$B_e = -\frac{ER^3}{2}.$$

With a nonconductive membrane surrounding a sphere, the induced transmembrane voltage is the opposite of the electric potential at the external surface of a homogeneous nonconductive sphere of equal size and orientation. Thus

$$\Delta\Phi(\varphi) = -\Phi(R, \varphi) = \frac{3}{2} ER \cos \varphi. \qquad (B.14)$$

C. A prolate spheroidal cell

With a prolate spheroid placed into a homogeneous electric field with the polar radius parallel to the electric field vector, we derive the spatial distribution of the electric potential in the prolate spheroidal coordinate system $\{(u, \nu, \vartheta) \in \mathbb{R}^3 : u \geq 0, 0 \leq \nu \leq \pi, 0 \leq \vartheta < 2\pi\}$ with the coordinates defined by

$$x = a \cosh u \cos \nu, \quad y = a \sinh u \sin \nu \cos \vartheta,$$

$$z = a \sinh u \sin \nu \sin \vartheta, \qquad (C.1)$$

where $2a$ is the distance between the foci.

For geometries with x-axial symmetry, the electric potential is independent of ϑ. We can then write $\Phi(u, \nu)$ instead of $\Phi(u, \nu, \vartheta)$, and Laplace's equation reads

$$\frac{\partial^2 \Phi}{\partial u^2} + \coth u \frac{\partial \Phi}{\partial u} + \frac{\partial^2 \Phi}{\partial \nu^2} + \cot \nu \frac{\partial \Phi}{\partial \nu} = 0. \quad (C.2)$$

The first such case is the electric potential distribution in uniform space. This distribution, which we denote by Φ_0, is linear, and for a field parallel to the x-axis it can be written in prolate spheroidal coordinates as

$$\Phi_0(u, \nu) = -Ea \cosh u \cos \nu. \qquad (C.3)$$

While a sphere is described solely by its radius, two parameters are needed to characterize a prolate spheroid, and there are two equivalent ways to accomplish this. In the first one, we define the distance a between the foci and the value U that describes the surface of the prolate spheroid for the chosen a as $u = U$. An alternative approach is to define the polar radius R_1 and the equatorial radius R_2 of the prolate spheroid. While the first characterization is better suited to the coordinate system, the second is more intuitive, as it resembles the characterization of a sphere. The two are bijectively related:

$$R_1 = a \cosh U; \quad R_2 = a \sinh U; \qquad (C.4)$$

$$a = \sqrt{R_1^2 - R_2^2}; \quad U = \operatorname{arctanh} \frac{R_2}{R_1} = \log \sqrt{\frac{R_1 + R_2}{R_1 - R_2}}. \quad (C.5)$$

We now place a prolate spheroid into the field so that its polar (i.e., larger) radius lies on the x-axis, and its center coincides with the origin of the coordinate system. Again, we have x-axial symmetry, and by solving for Φ in a separable form

$$\Phi(u, \nu) = G(u)H(\nu), \qquad (C.6)$$

Eq. C.2 becomes

$$\frac{G''(u) + \coth u\, G'(u)}{G(u)} = -\frac{H''(\nu) + \cot \nu\, H'(\nu)}{H(\nu)}. \qquad (C.7)$$

The left-hand side of Eq. C.7 is at any value of u equal to the right-hand side at any value of ν, which is only possible if they equal the same constant, which we denote by K. This splits Eq. C.7 into two ordinary differential equations

$$\begin{cases} G''(u) + \coth u\, G'(u) - KG(u) = 0 \\ H''(\nu) + \cot \nu\, H'(\nu) + KH(\nu) = 0 \end{cases} \qquad (C.8)$$

Far from the spheroid, the field is homogeneous and thus it follows from Eq. C.3 that $G(u) \propto \cosh u$. Such $G(u)$ is obtained from Eq. C.8 only if $K = 2$, and in that case

$$G(u) = C_1 \cosh u + C_2 \left(1 - \cosh u \log \sqrt{\frac{\cosh u + 1}{\cosh u - 1}} \right). \qquad (C.9)$$

$$H(\nu) = C_3 \cos \nu + C_4 \left(1 - \cos \nu \log \sqrt{\frac{1 + \cos \nu}{1 - \cos \nu}}\right). \tag{C.10}$$

with C_1, C_2, C_3, C_4 constants, of which C_4 must be zero, since $H(\nu)$ is continuous and bounded on $[0, \pi]$, and therefore

$$H(\nu) = C_3 \cos \nu. \tag{C.11}$$

We now join the functions given by Eqs. C.9 and C.11 according to Eq. C.6 and get

$$\Phi(u, \nu) = A \cosh u \cos \nu$$

$$+ B \left(1 - \cosh u \log \sqrt{\frac{\cosh u + 1}{\cosh u - 1}}\right) \cos \nu. \tag{C.12}$$

with A, B constants.

Since we treat the membrane as nonconductive, we proceed as described in the Methods section, looking for the electric potential distribution inside and outside a homogeneous nonconductive prolate spheroid. Let $u = U$ describe the surface of the prolate spheroid. Both inside and outside the spheroid, the electric potential distribution is given by a function of the general form of Eq. C.12, but with different values of A and B. We therefore write

$$\Phi(u, \nu)$$

$$= \begin{cases} \Phi_i(u, \nu) = A_i \cosh u \cos \nu \\ \quad + B_i \left(1 - \cosh u \log \sqrt{\frac{\cosh u + 1}{\cosh u - 1}}\right) \cos \nu; & 0 \leq u \leq U \\ \Phi_e(u, \nu) = A_e \cosh u \cos \nu \\ \quad + B_e \left(1 - \cosh u \log \sqrt{\frac{\cosh u + 1}{\cosh u - 1}}\right) \cos \nu; & U \leq u \end{cases}$$

$$\tag{C.13}$$

Applying the conditions of continuity and an additional assumption that $\sigma_m = 0$, we get the constants in Eq. C.13,

$$A_i = -\frac{Ea \operatorname{sech} U}{\cosh U - \log(\coth(U/2))\sinh^2 U}, \tag{C.14}$$

$$B_i = 0,$$

$$A_e = -Ea,$$

$$B_e = -\frac{Ea}{\log(\coth(U/2)) - \coth U \operatorname{csch} U}.$$

With a nonconductive membrane surrounding a prolate spheroid, the induced transmembrane voltage is the opposite of the electric potential at the external surface of a homogeneous nonconductive spheroid of equal shape and orientation. This gives

$$\Delta\Phi(\nu) = -\Phi(U, \nu)$$

$$= \frac{Ea}{\cosh U - \log(\coth(U/2))\sinh^2 U} \cos \nu. \tag{C.15}$$

To compare Eq. C.15 to its analog for a sphere given by Eq. 1, we must express the remaining variable, the coordinate ν, as a function of φ. There

is a bijective relation between the prolate spheroidal coordinates used in this section and spherical coordinates $(r, \varphi, \vartheta) \in \mathbb{R}^3$ used in Appendix B:

$$u(r, \varphi) = \Re\left(\operatorname{arccosh}\frac{re^{i\varphi}}{a}\right);$$

$$\nu(r, \varphi) = \Im\left(\operatorname{arccosh}\frac{re^{i\varphi}}{a}\right); \tag{C.16}$$

$$r(u, \nu) = a\sqrt{\frac{\cosh 2u + \cos 2\nu}{2}}; \tag{C.17}$$

$$\varphi(u, \nu) = \arctan(\cosh u \cos \nu, \sinh u \sin \nu).$$

Let $\mathcal{U}$ denote the surface of the prolate spheroid. There, r is related to φ as

$$r(\varphi)|_{\mathcal{U}} = \frac{R_1 R_2}{\sqrt{R_1^2 \sin^2\varphi + R_2^2\cos^2\varphi}}, \tag{C.18}$$

where R_1 is the polar, and R_2 the equatorial radius of the spheroid. Inserting this relation into Eq. C.16 and applying Eq. C.5, we can write the value of ν at the surface of $\mathcal{U}$ as

$$\nu(\varphi)|_{\mathcal{U}} = \Im\left(\operatorname{arccosh}\frac{R_1 R_2 e^{i\varphi}}{\sqrt{(R_1^2 - R_2^2)(R_1^2\sin^2\varphi + R_2^2\cos^2\varphi)}}\right). \tag{C.19}$$

After a trigonometric expansion of the complex term in Eq. C.19 and some calculation, we obtain

$$\nu(\varphi)|_{\mathcal{U}} = \arccos\frac{R_2\cos\varphi}{\sqrt{R_1^2\sin^2\varphi + R_2^2\cos^2\varphi}}. \tag{C.20}$$

It also follows from Eq. C.5 that

$$\frac{a}{\cosh U - \log(\coth(U/2))\sinh^2 U}$$

$$= \frac{R_1^2 - R_2^2}{R_1 - \frac{R_2^2}{\sqrt{R_1^2 - R_2^2}}\log\frac{R_1 + \sqrt{R_1^2 - R_2^2}}{R_2}}. \tag{C.21}$$

Introducing Eqs. C.20 and C.21 into Eq. C.15, we can now formulate in spherical coordinates the transmembrane voltage induced on a prolate spheroid

$$\Delta\Phi(\varphi) = E\frac{R_1^2 - R_2^2}{R_1 - \frac{R_2^2}{\sqrt{R_1^2 - R_2^2}}\log\frac{R_1 + \sqrt{R_1^2 - R_2^2}}{R_2}}\frac{R_2\cos\varphi}{\sqrt{R_1^2\sin^2\varphi + R_2^2\cos^2\varphi}}. \tag{C.22}$$

D. An oblate spheroidal cell

With an oblate spheroid placed into a homogeneous electric field with the polar radius parallel to the electric field vector, we derive the spatial distribution of the electric potential in the oblate spheroidal coordinate system $\{(u, \nu, \vartheta) \in \mathbb{R}^3 : w \geq 0, 0 \leq \eta \leq \pi, 0 \leq \vartheta < 2\pi\}$ with the

coordinates defined by

$$x = a \sinh w \cos \eta,$$

$$y = a \cosh w \sin \eta \cos \vartheta, \qquad (D.1)$$

$$z = a \cosh w \sin \eta \sin \vartheta,$$

where $2a$ is the distance between the foci.

For geometries with x-axial symmetry, the electric potential is independent of ϑ. We can then write $\Phi(w, \eta)$ instead of $\Phi(w, \eta, \vartheta)$, and the Laplace's equation reads

$$\frac{\partial^2 \Phi}{\partial w^2} + \tanh w \frac{\partial \Phi}{\partial w} + \frac{\partial^2 \Phi}{\partial \eta^2} + \cot \eta \frac{\partial \Phi}{\partial \eta} = 0. \quad (D.2)$$

The first such case is the electric potential distribution in uniform space. This distribution, which we denote by Φ_0, is linear, and for a field parallel to the x-axis it can be written in oblate spheroidal coordinates as

$$\Phi_0(w, \eta) = -Ea \sinh w \cos \eta \qquad (D.3)$$

As with a prolate spheroid, two parameters are needed to characterize an oblate spheroid, and this can be accomplished either by defining the distance a between the foci and the surface of the oblate spheroid (for the chosen a) as $w = W$, or by the polar radius R_1 and the equatorial radius R_2 of the oblate spheroid. The two characterizations are bijectively related:

$$R_1 = a \sinh W; \quad R_2 = a \cosh W; \qquad (D.4)$$

$$a = \sqrt{R_2^2 - R_1^2}; \quad W = \operatorname{arctanh} \frac{R_1}{R_2} = \log \sqrt{\frac{R_1 + R_2}{R_2 - R_1}}. \quad (D.5)$$

We now place an oblate spheroid into the field so that its polar (i.e., smaller) radius lies on the x-axis, and its center coincides with the origin of the coordinate system. Again, we have x-axial symmetry, and by solving for Φ in a separable form

$$\Phi(w, \eta) = G(w)H(\eta), \qquad (D.6)$$

Eq. D.2 becomes

$$\frac{G''(w) + \tanh w\, G'(w)}{G(w)} = -\frac{H''(\eta) + \cot \eta\, H'(\eta)}{H(\eta)}. \quad (D.7)$$

The left-hand side of Eq. D.7 is at any value of w equal to the right-hand side at any value of η, which is only possible if they equal the same constant, which we denote by K. This splits Eq. D.7 into two ordinary differential equations

$$\begin{cases} G''(w) + \tanh w\, G'(w) - KG(w) = 0 \\ H''(\eta) + \cot \eta\, H'(\eta) + KH(\eta) = 0 \end{cases} \qquad (D.8)$$

Far from the spheroid, the field is homogeneous and thus it follows from D.3 that $G(w) \propto \sinh w$. Such $G(w)$ is obtained from Eq. D.8 only if $K = 2$, and in that case

$$G(w) = C_1 \sinh w + C_2(\sinh w \operatorname{arccot}(\sinh w) - 1). \qquad (D.9)$$

$$H(\eta) = C_3 \cos \eta + C_4\left(1 - \cos \eta \log \sqrt{\frac{1 + \cos \eta}{1 - \cos \eta}}\right). \qquad (D.10)$$

with C_1, C_2, C_3, C_4 constants, of which C_4 must be zero, since $H(\eta)$ is continuous and bounded on $[0, \pi]$, and therefore

$$H(\eta) = C_3 \cos \eta. \qquad (D.11)$$

We now join the functions given by Eqs. D.9 and D.11 according to Eq. D.6 and get

$$\Phi(w, \eta) = A \sinh w \cos \eta$$
$$+ B(\sinh w \operatorname{arccot}(\sinh w) - 1)\cos \eta. \qquad (D.12)$$

with A, B constants.

Since we treat the membrane as nonconductive, we proceed as described in the Methods section, looking for the electric potential distribution inside and outside a homogeneous nonconductive oblate spheroid. Let $w = W$ describe the surface of the oblate spheroid. Both inside and outside the spheroid, the electric potential distribution is given by a function of the general form (D.12), but with different values of A and B. We therefore write

$$\Phi(w, \eta)$$

$$= \begin{cases} \Phi_i(w, \eta) = A_i \sinh w \cos \eta & 0 \le w \le W \\ \qquad\qquad + B_i(\sinh w \operatorname{arccot}(\sinh w) - 1)\cos \eta; \\ \Phi_e(w, \eta) = A_e \sinh w \cos \eta & W \le w \\ \qquad\qquad + B_e(\sinh w \operatorname{arccot}(\sinh w) - 1)\cos \eta; \end{cases}$$

$$(D.13)$$

Applying the conditions of continuity and an additional assumption that $\sigma_m = 0$, we get the constants in Eq.D.13,

$$A_i = -\frac{Ea \operatorname{csch} W}{\operatorname{arccot}(\sinh W)\cosh^2 W - \sinh W},$$

$$B_i = 0, \qquad (D.14)$$

$$A_e = -Ea,$$

$$B_e = -\frac{Ea}{\tanh W \operatorname{sech} W - \operatorname{arccot}(\sinh W)}.$$

With a nonconductive membrane surrounding an oblate spheroid, the induced transmembrane voltage is the opposite of the electric potential at the external surface of a homogeneous nonconductive spheroid of equal shape and orientation. This gives

$$\Delta\Phi(\eta) = -\Phi(W, \eta)$$

$$= \frac{Ea}{\operatorname{arccot}(\sinh W)\cosh^2 W - \sinh W} \cos \eta. \quad (D.15)$$

To compare Eq. D.15 to its analog for a sphere given by Eq. 1, we must express the remaining variable, the coordinate η, as a function of φ. There is a bijective relation between the oblate spheroidal coordinates used in this section and spherical coordinates $(r, \varphi, \vartheta) \in \mathbb{R}^3$ used in Appendix B:

$$w(r, \varphi) = \Re\left(\operatorname{arccosh} \frac{ire^{i\varphi}}{a}\right);$$

$$(D.16)$$

$$\eta(r, \varphi) = \frac{\pi}{2} - \Im\left(\operatorname{arccosh} \frac{ire^{i\varphi}}{a}\right);$$

$$r(w, \eta) = a\sqrt{\frac{\cosh 2w - \cos 2\eta}{2}}; \tag{D.17}$$

$$\varphi(w, \eta) = \arctan(\sinh w \cos \eta, -\cosh w \sin \eta).$$

Let $\mathcal{W}$ denote the surface of the oblate spheroid. There, r is related to φ as

$$r(\varphi)|_{\mathcal{W}} = \frac{R_1 R_2}{\sqrt{R_1^2 \sin^2\varphi + R_2^2\cos^2\varphi}}, \tag{D.18}$$

where R_1 is the larger, and R_2 the smaller radius of the spheroid. Inserting this relation into Eq. D.16 and applying Eq. D.5, we can write the value of η at the surface $\mathcal{W}$ as

$$\eta(\varphi)|_{\mathcal{W}} = \frac{\pi}{2}$$

$$- \Im\left(\operatorname{arccosh} \frac{iR_1 R_2 e^{i\varphi}}{\sqrt{(R_2^2 - R_1^2)(R_1^2 \sin^2\varphi + R_2^2 \cos^2\varphi)}}\right). \tag{D.19}$$

After a trigonometric expansion of the complex term in Eq. D.19 and some calculation, we obtain

$$\eta(\varphi)|_{\mathcal{W}} = \frac{\pi}{2} - \arcsin\frac{R_2\cos\varphi}{\sqrt{R_1^2 \sin^2\varphi + R_2^2 \cos^2\varphi}}$$

$$= \arccos\frac{R_2\cos\varphi}{\sqrt{R_1^2 \sin^2\varphi + R_2^2 \cos^2\varphi}}. \tag{D.20}$$

It also follows from Eq. D.5 that

$$\frac{a}{\operatorname{arccot}(\sinh W)\cosh^2 W - \sinh W}$$

$$= \frac{R_2^2 - R_1^2}{\dfrac{R_2^2}{\sqrt{R_2^2 - R_1^2}} \operatorname{arccot} \dfrac{R_1}{\sqrt{R_2^2 - R_1^2}} - R_1}. \tag{D.21}$$

Introducing Eqs. D.20 and D.21 into Eq. D.15, we can now formulate in spherical coordinates the transmembrane voltage induced on an oblate spheroid

$$\Delta\Phi(\varphi)$$

$$= E\frac{R_2^2 - R_1^2}{\dfrac{R_2^2}{\sqrt{R_2^2 - R_1^2}} \operatorname{arccot} \dfrac{R_1}{\sqrt{R_2^2 - R_1^2}} - R_1} \frac{R_2\cos\varphi}{\sqrt{R_1^2 \sin^2\varphi + R_2^2 \cos^2\varphi}}.$$

$$\tag{D.22}$$

REFERENCES

Bernhardt, J., and H. Pauly. 1973. On the generation of potential differences across the membranes of ellipsoidal cells in an alternating electrical field. *Biophysik.* 10:89–98.

Bryant, G., and J. Wolfe. 1987. Electromechanical stresses produced in the plasma membranes of suspended cells by applied electric fields. *J. Membr. Biol.* 96:129–139.

Eisenhart, L. P. 1934. Separable systems of Stäckel. *Ann. Math.* 35:284–305.

Gimsa, J., and D. Wachner. 1999. A polarization model overcoming the geometric restrictions of the Laplace solution for spheroidal cells: obtaining new equations for field-induced forces and transmembrane potential. *Biophys. J.* 77:1316–1326.

Grosse, C., and H. P. Schwan. 1992. Cellular membrane potentials induced by alternating fields. *Biophys. J.* 63:1632–1642.

Jerry, R. A., A. S. Popel, and W. E. Brownell. 1996. Potential distribution for a spheroidal cell having a conductive membrane in an electric field. *IEEE Trans. Biomed. Eng.* 43:970–972.

Klee, M., and R. Plonsey. 1972. Finite difference solution for biopotentials of axially symmetric cells. *Biophys. J.* 12:1661–1675.

Klee, M., and R. Plonsey. 1976. Stimulation of spheroidal cells—the role of cell shape. *IEEE Trans. Biomed. Eng.* 23:347–354.

Kotnik, T., F. Bobanović, and D. Miklavčič. 1997. Sensitivity of transmembrane voltage induced by applied electric fields—a theoretical analysis. *Bioelectrochem. Bioenerg.* 43:285–291.

Kotnik, T., T. Slivnik, and D. Miklavčič. 1998. Time course of transmembrane voltage induced by time-varying electric fields—a method for theoretical analysis and its application. *Bioelectrochem. Bioenerg.* 45:3–16.

Morse, P. M., and H. Feshbach. 1953. Methods of Theoretical Physics, Part I. McGraw-Hill, New York. 656–666.

Neumann, E., and S. Kakorin. 1996. Electrooptics of membrane electroporation and vesicle shape deformation. *Curr. Opin. Colloid Interface Sci.* 1:790–799.

Neumann, E., S. Kakorin, and K. Toensing. 1999. Fundamentals of electroporative delivery of drugs and genes. *Bioelectrochem. Bioenerg.* 48:3–16.

Rand, R. P. 1964. Mechanical properties of the red blood cell membrane. II. Viscoelectric breakdown of the membrane. *Biophys. J.* 4:303–316.

Schwan, H. P. 1957. Electrical properties of tissue and cell suspensions. *Adv. Biol. Med. Phys.* 5:147–209.

Winterhalter, M., and W. Helfrich. 1988. Deformation of spherical vesicles by electric fields. *J. Colloid Interface Sci.* 122:583–586.

Wolfe, J., M. F. Dowgert, and P. L. Steponkus. 1986. Mechanical study of the deformation and rupture of the plasma membranes of protoplasts during osmotic expansion. *J. Membr. Biol.* 93:63–74.